Simplified models for dark matter face their consistent completions

Dorival Gonçalves,[1,2,*] Pedro A. N. Machado,[3,4,†] and Jose Miguel No[5,6,‡]

[1]*Institute of Particle Physics Phenomenology, Physics Department, Durham University, Durham DH1 3LE, United Kingdom*

[2]*Department of Physics and Astronomy, University of Pittsburgh, 3941 O'Hara Street, Pittsburgh, Pennsylvania 15260, USA*

[3]*Instituto de Fisica Teorica IFT-UAM/CSIC, Universidad Autonoma de Madrid Cantoblanco, 28049 Madrid, Spain*

[4]*Theoretical Physics Department, Fermi National Accelerator Laboratory, Batavia, Illinois 60510, USA*

[5]*Department of Physics and Astronomy, University of Sussex, Brighton BN1 9QH, United Kingdom*

[6]*Department of Physics, King's College London, Strand, WC2R 2LS London, United Kingdom*

(Received 1 December 2016; published 30 March 2017)

Simplified dark matter models have been recently advocated as a powerful tool to exploit the complementarity between dark matter direct detection, indirect detection and LHC experimental probes. Focusing on pseudoscalar mediators between the dark and visible sectors, we show that the simplified dark matter model phenomenology departs significantly from that of consistent $SU(2)_{\rm L} \times U(1)_{\rm Y}$ gauge invariant completions. We discuss the key physics that simplified models fail to capture, and its impact on LHC searches. Notably, we show that resonant mono-Z searches provide competitive sensitivities to standard mono-jet analyses at 13 TeV LHC.

DOI: 10.1103/PhysRevD.95.055027

I. INTRODUCTION

The nature of dark matter (DM) is an outstanding mystery at the interface of particle physics and cosmology. At the core of the current paradigm, is the well-motivated Weakly-Interacting-Massive-Particle (WIMP), a thermal relic in the GeV-TeV mass range (see [1] for a review). WIMPs may pertain to a hidden sector, neutral under the Standard Model (SM) gauge group and interacting with the SM via a *portal* [2].

The large experimental effort aimed at revealing the nature of DM and its interactions with the SM proceeds along three main avenues: (i) Low energy direct detection experiments, which measure the scattering of ambient DM from heavy nuclei. (ii) Indirect detection experiments which measure the energetic particles product of DM annihilations in space. (iii) DM searches at the Large Hadron Collider (LHC), where pairs of DM particles could be produced and manifest themselves as events showing an imbalance in momentum conservation (through the presence of missing transverse momentum $\not{E}_T$ recoiling against a visible final state).

The complementarity of different DM search avenues plays a very important role in the exploration of DM properties, and thus approaches which allow to fully exploit such complementarity have received a great deal of attention [3–8]. The leading two such approaches are effective field theories (EFTs) and DM simplified models. The latter have increasingly gained attention as, at the LHC, large missing energy selections render the EFT invalid for a significant range of the parameter space [9–11].

However, it is crucial that the simplified models do correctly describe the relevant physics that a realistic theory beyond the SM would yield at the LHC, direct and indirect detection experiments, at least in some limit. In this paper, we show that for simplified DM models with a pseudoscalar mediator, the minimal consistent $SU(2)_{\rm L} \times U(1)_{\rm Y}$ gauge invariant completions to which these simplified models may be mapped yield a very different physical picture, signaling a failure of the simplified models to capture part of the key DM physics: these models are "oversimplified" (see [12–19] for recent discussions on this issue). We detail the physics that such simplified models are neglecting, and show that it has a critical impact on DM searches at the LHC. Particularly, we demonstrate that the resonant mono-Z channel displays competitive sensitivities to the usual mono-jet analysis at the LHC Run-II.

II. SIMPLIFIED PSEUDOSCALAR PORTAL FOR DARK MATTER

The simplified model DM scenario that we consider consists of a gauge singlet DM fermion χ (for concreteness we assume a Dirac fermion). Our results can be easily generalized to Majorana fermions [5]), whose interactions with the SM occur via a pseudoscalar mediator a [4,20–24], namely

*dorival.goncalves@pitt.edu
†pmachado@fnal.gov
‡j.m.no@sussex.ac.uk

$$\mathcal{L}_s = \bar{\chi}(i\partial\!\!\!/ - m_\chi)\chi + \frac{1}{2}(\partial_\mu a)^2 - \frac{m_a^2}{2}a^2 - g_\chi a\bar{\chi}i\gamma^5\chi - g_{\rm SM}a\sum_f \frac{y_f}{\sqrt{2}}\bar{f}i\gamma^5 f. \quad (1)$$

We emphasize that a built-in assumption in these scenarios is that DM belongs to a hidden sector, neutral under SM gauge interactions.[1] The model in Eq. (1) is described in terms of four parameters: the masses for the DM m_χ and the mediator m_a, a nd the couplings of the mediator to DM g_χ and the SM[2] $g_{\rm SM}$. Assuming the DM candidate χ to be a thermal relic which obtains its abundance via freeze-out, the relevant early Universe annihilation channels for χ are into bottom quarks (for $m_\chi > m_b$), top quarks (for $m_\chi > m_t$) and mediators (for $m_\chi > m_a$). The respective thermally averaged annihilation cross sections are

$$\langle\sigma{\rm v}\rangle_{\bar{f}f} = \frac{3g_\chi^2 g_{\rm SM}^2 m_f^2}{4\pi v^2}\frac{m_\chi^2\sqrt{1-\frac{m_f^2}{m_\chi^2}}}{(m_a^2-4m_\chi^2)^2+m_a^2\Gamma_a^2},$$
$$\langle\sigma{\rm v}\rangle_{aa} = \frac{g_\chi^4(1-\frac{m_a^2}{m_\chi^2})^{3/2}}{8m_\chi^2(2-\frac{m_a^2}{m_\chi^2})^2}, \quad (2)$$

where $v = 246$ GeV. We note that the observed DM relic abundance is obtained for $\langle\sigma{\rm v}\rangle \simeq 3\times10^{-26}$ cm^3/s.

Concerning DM direct detection, the pseudoscalar portal yields a spin-dependent and spin-independent cross section respectively at tree-level and one-loop. The experimental constraints are overall found to be extremely weak [25], and so we can safely disregard DM direct detection in the following discussion. We also postpone a detailed discussion of indirect detection constraints for the future [26] and focus in this work on DM relic density and collider searches.

III. GAUGE-INVARIANT MODELS: PSEUDOSCALAR MEDIATOR

A consistent realization of the simplified model scenario displayed in Eq. (1), respecting $SU(2)_{\rm L}\times U(1)_{\rm Y}$ gauge invariance, is obtained along the following two possible avenues:

(i) Extending the SM scalar sector with a field that couples to SM fermions and yields pseudoscalar mixing with the real mediator field a.

(ii) Allowing the SM fermions to mix with heavy vectorlike fermion partners ψ, which couple to the pseudoscalar mediator a via $g_a a\bar{\psi}i\gamma^5\psi$.

In the latter case, the couplings between a and the SM fermions are weighted by the Yukawa couplings y_f as in the simplified model Eq. (1), and the $g_{{\rm SM},i}$ parameter (one for each SM fermion) is related to the product of the fermion mixing and g_a. In this scenario the top/bottom partner mixing plays the most important role, and the model needs to incorporate a custodial symmetry to comply with constraints from electroweak precision observables, particularly the Zbb coupling and the T parameter. The phenomenology of such scenarios will be studied in a future manuscript [26].

In this work we analyze in detail the former scenario, hereinafter referred to as pseudoscalar portal mixing scenario. The dark sector Lagrangian, in terms of the DM χ and pseudoscalar mediator a_0, both $SU(2)_{\rm L}\times U(1)_{\rm Y}$ singlets, is simply written as

$$V_{\rm dark} = \frac{m_{a_0}^2}{2}a_0^2 + m_\chi\bar{\chi}\chi + g_\chi a_0\bar{\chi}i\gamma^5\chi. \quad (3)$$

We extend the SM Higgs sector to include two scalar doublets $H_{1,2}$ [27]. The scalar potential for the two Higgs doublets, assuming CP-conservation and a softly broken $\mathbb{Z}_2$ symmetry, reads

$$V_{\rm 2HDM} = \mu_1^2|H_1|^2 + \mu_2^2|H_2|^2 - \mu^2[H_1^\dagger H_2 + {\rm H.c.}] + \frac{\lambda_1}{2}|H_1|^4 + \frac{\lambda_2}{2}|H_2|^4 + \lambda_3|H_1|^2|H_2|^2 + \lambda_4|H_1^\dagger H_2|^2 + \frac{\lambda_5}{2}[(H_1^\dagger H_2)^2 + {\rm H.c.}], \quad (4)$$

and the portal between visible and hidden sectors occurs via $V_{\rm portal} = i\kappa a_0 H_1^\dagger H_2 + {\rm H.c.}$ [25,27,28]. The two doublets are $H_i = (\phi_i^+, (v_i + h_i + \eta_i)/\sqrt{2})^T$, with v_i their vev ($\sqrt{v_1^2+v_2^2} = v$, $v_2/v_1 \equiv \tan\beta = t_\beta$). The scalar spectrum contains a charged scalar $H^\pm = c_\beta\phi_2^\pm - s_\beta\phi_1^\pm$ ($c_\beta \equiv \cos\beta$, $s_\beta \equiv \sin\beta$) and two neutral CP-even scalars $h = c_\alpha h_2 - s_\alpha h_1$, $H = -s_\alpha h_2 - c_\alpha h_1$, with h identified as the 125 GeV Higgs state (SM-like in the alignment limit $\beta-\alpha = \pi/2$ [29]). The neutral CP-odd scalar $A_0 = c_\beta\eta_2 - s_\beta\eta_1$ mixes with a_0 for $\kappa \neq 0$, yielding two pseudoscalar mass eigenstates a, A (with $m_A > m_a$): $A = c_\theta A_0 + s_\theta a_0$, $a = c_\theta a_0 - s_\theta A_0$. In terms of the mass eigenstates, we get

$$V_{\rm dark} \supset g_\chi(c_\theta a + s_\theta A)\bar{\chi}i\gamma^5\chi,$$
$$V_{\rm portal} = \frac{(m_A^2-m_a^2)s_{2\theta}}{2v}(c_{\beta-\alpha}H - s_{\beta-\alpha}h) \times [aA(s_\theta^2-c_\theta^2) + (a^2-A^2)s_\theta c_\theta]. \quad (5)$$

[1]Departing from this assumption would dramatically modify DM phenomenology at the LHC, direct and indirect DM detection experiments.

[2]The models assume a Minimal Flavor Violation scenario. A universal rescaling $g_{\rm SM}$ can be generalized within the simplified model framework.

The coupling of the pseudoscalar mediators a, A to the SM fermions occurs via the Yukawa couplings of the scalar doublets $H_{1,2}$. We consider a scenario with all SM fermions coupled to the same doublet (2HDM Type I), and another with down-type and up-type quarks coupled to different doublets (2HDM Type II) (see e.g. [30] for details). In the first case, the couplings of a (A) to SM fermions are all weighted by $s_\theta t_\beta^{-1}$ ($c_\theta t_\beta^{-1}$). In the second scenario, the weight is $s_\theta t_\beta^{-1}$ ($c_\theta t_\beta^{-1}$) for up-type quarks and $s_\theta t_\beta$ ($c_\theta t_\beta$) for down-type quarks. We note that for Type II the alignment limit $c_{\beta-\alpha} = 0$ is favored [31], and thus this scenario will be considered in the rest of this paper. The new scalars also impact electroweak precision observables [32], and we fix in the following $m_{H^\pm} \simeq m_H$ to satisfy T-parameter bounds [33].

We now confront the pseudoscalar portal mixing scenario with the simplified model pseudoscalar portal in Eq. (1). First, we note that the portal interaction can be rewritten as

$$\kappa = \frac{m_A^2 - m_a^2}{2v} s_{2\theta}. \tag{6}$$

The presence of the portal between the visible and dark sectors ($\kappa \neq 0$) then implies a nonzero mixing $s_{2\theta} \neq 0$. As outlined above, this mixing allows the pseudoscalar mediator a to couple to SM fermions ($g_{\rm SM} \neq 0$), as is needed for the simplified model construct to be of any phenomenological relevance.[3] For fixed $s_{2\theta}$ the portal interaction grows larger as the mass of A increases. The unitarity of scattering processes aa, AA, $aA \to W^+W^-$ yields an upper bound on $\Delta_a^2 = m_A^2 - m_a^2$, leading to a nondecoupling of the states A, H and $H^\pm$. We compute the scattering amplitude matrix $\mathcal{M}_{ij\to WW}$ ($i, j = a, A$), choosing $c_{\beta-\alpha} = 0$ as a conservative assumption since the unitarity bounds are stronger away from alignment. The amplitudes read in this limit

$$\mathcal{M}_{AA\to WW} = \frac{g^2}{2} c_\theta^2 \left(\frac{\Delta_H^2}{m_W^2} + \frac{\Delta_a^2 (1 - c_\theta^2)}{2 m_W^2} \right), \tag{7}$$

$$\mathcal{M}_{Aa\to WW} = -\frac{g^2}{2} s_\theta c_\theta \left(\frac{\Delta_H^2}{m_W^2} - \frac{\Delta_a^2 (\frac{1}{2} - s_\theta^2)}{2 m_W^2} \right), \tag{8}$$

$$\mathcal{M}_{aa\to WW} = \frac{g^2}{2} s_\theta^2 \left(\frac{\Delta_H^2}{m_W^2} - \frac{3 \Delta_a^2 c_\theta^2}{2 m_W^2} \right), \tag{9}$$

with $\Delta_H^2 = M^2 - m_{H^\pm}^2 + 2m_W^2 - m_h^2/2$, $M^2 \equiv \mu^2/(s_\beta c_\beta)$, neglecting $\mathcal{O}(1/t, 1/s)$ terms. The eigenvalues of the scattering amplitude matrix are given by

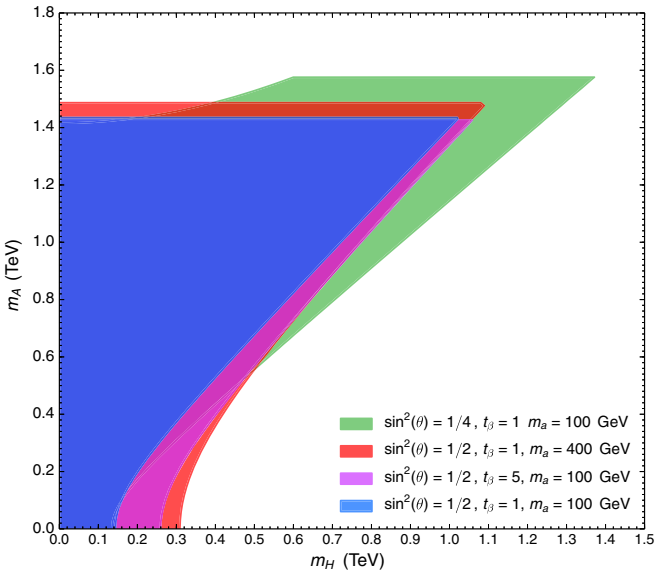

FIG. 1. Allowed parameter space in the (m_H, m_A) from unitarity and stability constraints (see text for details).

$$\Lambda_\pm = \left[\frac{\Delta_H^2}{v^2} - \frac{\Delta_a^2 (1 - c_{4\theta})}{8v^2} \pm \sqrt{\frac{\Delta_H^4}{v^4} + \frac{\Delta_a^4 (1 - c_{4\theta})}{8v^4}} \right], \tag{10}$$

and the unitarity bound on the scattering processes aa, AA, $aA \to W^+W^-$ is given by $|\Lambda_\pm| \leq 8\pi$. In addition, a set of unitarity bounds restrict the values of the quartic interactions in Eq. (4) [34–37], which in combination with boundness from below conditions on the scalar potential limits the allowed parameter ranges (see e.g. the discussion in [38,39]). The combination of bounds yields an allowed region in the (m_H, m_A) mass plane, weakly dependent on m_a and t_β, as shown in Fig. 1. While the allowed region increases as s_θ decreases, Fig. 1 shows that the states A, $H^\pm$, H cannot be heavier than $\mathcal{O}(\text{TeV})$ if the portal between visible and dark sectors is active.

We now compare the DM phenomenology of the simplified model and the consistent completion, with particular emphasis on the phenomenological impact of the new states A, $H^\pm$, H present in the consistent completion.

A. Dark matter relic density

In order not to overclose the universe, a minimum value of the coupling $g_{\rm SM}$ between a and the SM fermions is required. This yields a minimum value of the mixing s_θ for a fixed t_β value.[4] At the same time, charged scalar loop contributions to the $\bar{B} \to X_s\gamma$ flavor process [40,41] on the $(m_{H^\pm}, t_\beta)$ plane yield a lower limit on t_β. $H^\pm$ cannot be heavier than $\mathcal{O}(\text{TeV})$ from unitarity arguments. Requiring

[3]For $g_{\rm SM} = 0$, the observed DM relic abundance could still be obtained via $\bar{\chi}\chi \to aa$ annihilations (for $m_\chi > m_a$). However, in this case there would be no direct, indirect or LHC DM signatures.

[4]We recall that for Type I (Type II) $g_{\rm SM} = s_\theta t_\beta^{-1}$ ($g_{\rm SM} = s_\theta t_\beta^{-1}$ for t quarks and $g_{\rm SM} = s_\theta t_\beta$ for b quarks).

$m_{H^\pm} < 1$ TeV results in the bound $t_\beta \gtrsim 0.8$ for 2HDM Type I, which then translates into an upper bound on $g_{\rm SM}$. Similar upper (lower) bounds on $g_{\rm SM}$ from the lower $\bar{B} \to X_s\gamma$ bound on t_β apply for 2HDM Type II when the DM annihilates dominantly into top (bottom) quarks.

Besides these constraints on $g_{\rm SM}$ which are not present in the simplified model, another key difference between the consistent completion and the simplified model is the presence of new DM annihilation channels $\bar{\chi}\chi \to ah, Zh$ (the latter for $c_{\beta-\alpha} \neq 0$), which can be the dominant DM annihilation process for heavy DM and light a. Particularly, the annihilation into ah is maximal in the alignment limit $c_{\beta-\alpha} = 0$, for which the cross section reads

$$\langle\sigma v\rangle_{ah} = \frac{g_\chi^2 s_{2\theta}^2}{64\pi^2 v^2}\sqrt{1-\frac{(m_a+m_h)^2}{4m_\chi^2}}(m_A^2-m_a^2)^2 \times\left(\frac{c_\theta s_{2\theta}}{2(m_a^2-4m_\chi^2)}-\frac{s_\theta c_{2\theta}}{(m_A^2-4m_\chi^2)}\right)^2. \quad (11)$$

The relic density comparison between simplified model and consistent completion discussed above is illustrated in Fig. 2, where the value of $g_{\rm SM}$ required to yield $\langle\sigma v\rangle \simeq 3\times10^{-26}$ cm^3/s for simplified model and consistent completion is shown respectively in dashed and solid lines, for 2HDM Type I (Fig. 2 upper) and Type II (Fig. 2 lower) in the $(m_a, g_{\rm SM})$ plane. In each case, we consider as illustration $m_\chi = 80$ GeV, below the $\bar{t}t$ annihilation threshold with $\bar{\chi}\chi \to \bar{b}b$ becoming important, and $m_\chi = 200$ GeV, above the $\bar{t}t$ annihilation threshold. To understand the features of these curves, consider e.g. the $m_\chi = 80$ GeV scenario for Type II 2HDM (Fig. 2, bottom-left). When $m_a > 2m_\chi = 160$ GeV, the value of $g_{\rm SM}$ required to yield the relic abundance annihilation cross section is quite large, and the $\langle\sigma v\rangle$ predictions for simplified model and consistent completion coincide (dashed and solid lines are on top of each other in Fig. 2). As $m_a \to 2m_\chi$, the $\bar{\chi}\chi \to \bar{b}b$ process becomes resonant (modulated by the narrow width of a) resulting in a much smaller value of $g_{\rm SM}$. For $m_a < m_\chi$, the t-channel annihilation process $\bar{\chi}\chi \to aa$ opens up, and the required value of $g_{\rm SM}$ decreases again. Finally, in the consistent completion the annihilation channel $\bar{\chi}\chi \to ah$ becomes avaliable for $m_\chi > (m_a+m_h)/2$, not being present in the simplified model. This leads to a depletion of the relic abundance in the consistent completion since $\langle\sigma v\rangle_{ah} > 3\times10^{-26}$ cm^3/s (regardless of the value of $g_{\rm SM}$), yielding the sharp kink observed in the solid-red line. In contrast, the simplified model continues to yield the observed relic abundance for $m_\chi > (m_a+m_h)/2$, via $\bar{\chi}\chi \to aa$ annihilation.

As highlighted in Fig. 2, for 2HDM Type I and $m_\chi < m_t$, the t_β flavor bound constrains the consistent completion to the resonant $\bar{\chi}\chi \to \bar{b}b$ annihilation region or to the region $m_\chi \gtrsim m_a$ where the new annihilation channels $\bar{\chi}\chi \to ah$, Zh may be important. No such constraint is present in the simplified model. Above the top-quark threshold, simplified model and consistent completion yield the same result both for 2HDM Type I and II, except again for $m_\chi > (m_a+m_h)/2$ and/or $c_{\beta-\alpha} \neq 0$ (with $\bar{\chi}\chi \to Zh$ open) where the new channels play a key role. It also follows from this discussion that indirect DM detection in the gauge-invariant completion and the simplified model may differ significantly [26]. However, we show in the following that it is in the context of LHC searches where the difference between simplified model and consistent completion becomes crucial.

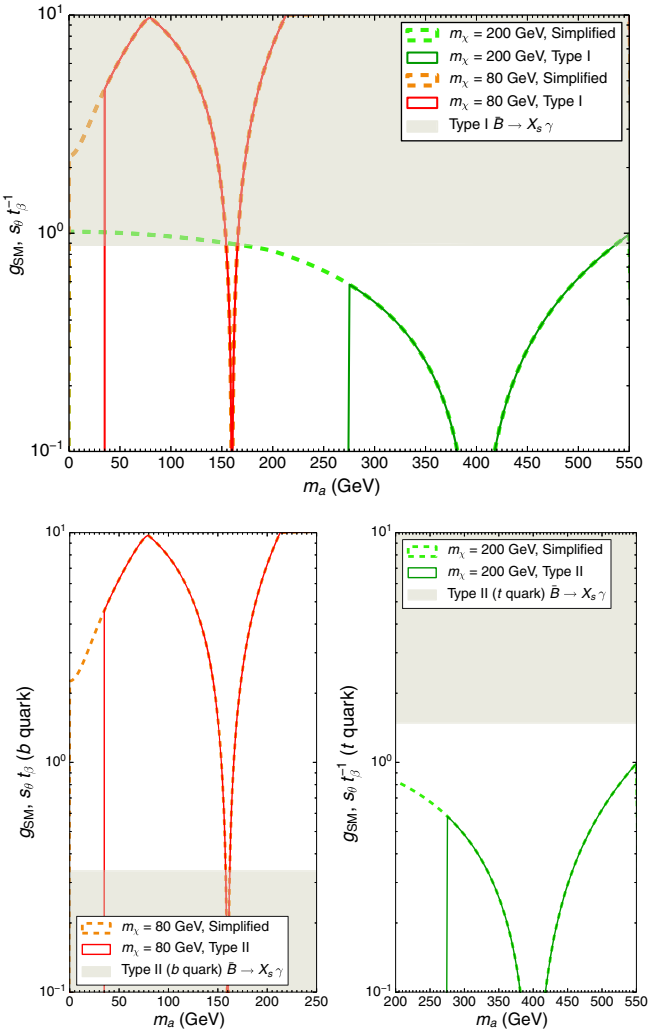

FIG. 2. Relic density comparison between simplified model and 2HDM Type I (upper panel) and Type II (lower panels) completion for $\sin^2(\theta)=1/2$, $m_{H^\pm}=m_H=1$ TeV, $m_A = 1.4$ TeV, $g_\chi = 0.15$, $c_{\beta-\alpha} = 0$.

B. LHC phenomenology: Mono-jet searches

We first study the collider phenomenology of the pseudoscalar resonances for "mono-jets" searches, $pp \to a +$ jets. The canonical signal is defined by the

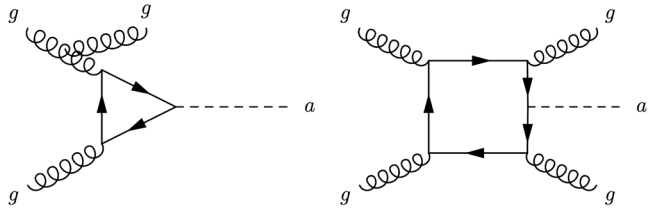

FIG. 3. Feynman diagrams for $pp \to a +$ jets production with up to two extra jets.

presence of large missing energy, from the pseudoscalar decay to DM, $a \to \bar{\chi}\chi$, recoiling against one or more jets. A sample of Feynman diagrams contributing to the signal is shown in Fig. 3.

For our analysis, we generate the signal sample with SHERPA+OPENLOOPS [42,43], merging up to two extra jets via the CKKW algorithm [44] and accounting for the heavy quark mass effects to the pseudoscalar production. Notably, these mass effects result in relevant changes to the $\not{E}_T$ distribution above m_t [4,45,46], precisely the most sensitive region for the mono-jet search. We include next-to-leading order (NLO) QCD corrections through the scaling factor $K \sim 1.5$ [45]. Hadronization and underlying event effects are also simulated.

Following the recent 13 TeV CMS $\not{E}_T +$ jets analysis [47], we define jets with the anti-k_T algorithm $R = 0.4$, $p_T^j > 30$ GeV and $|\eta_j| < 2.5$ via FASTJET [48]. b-jets are vetoed with 70% b-tagging efficiency and 1% mistag rate [49]. Electrons and muons with $p_T^\ell > 10$ GeV and

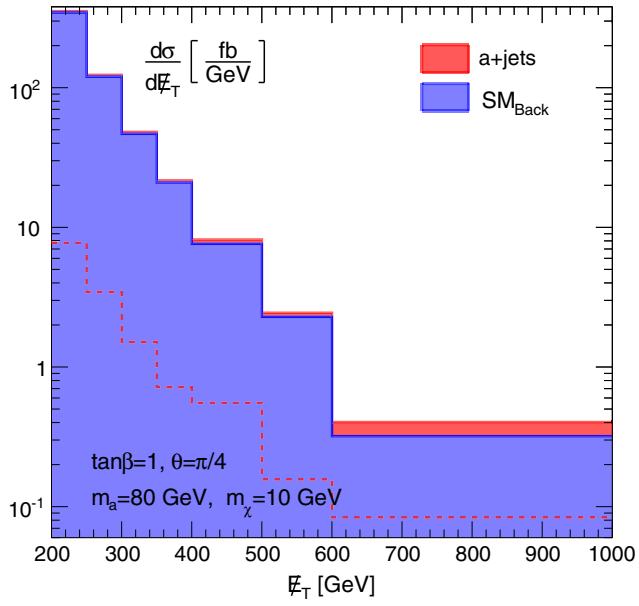

FIG. 4. Signal (red) and background (blue) transverse missing energy $\not{E}_T$ distributions. Shaded (empty) histograms are (non) stacked. We assume $m_\chi = 10$ GeV, $\sin^2\theta = 1/2$, $\tan\beta = g_\chi = 1$ and $m_a = 80$ GeV (with $m_A \gg m_a$). The SM background was obtained from [47].

$|\eta_\ell| < 2.5$ are rejected. To suppress the $Z +$ jets background, events are selected with $p_T^{j_1} > 100$ GeV for the leading jet and $\not{E}_T > 200$ GeV. Finally, to further reduce the multi-jet background, the azimuthal angle between the $\not{E}_T$ direction and the first four leading jets is required to be > 0.5. To validate our analysis implementation, we have generated the same signal considered by Ref. [47], vector mediator (V) plus jets, assuming $m_V = 1$ TeV with POWHEG [50,51]. We observe the same signal acceptance quoted by the experimental publication ~2%.

In Fig. 4, we show the $\not{E}_T$ distribution for the signal with $m_a = 80$ GeV. The sum of SM backgrounds was obtained from [47], which accounts for $Z +$ jets, $W +$ jets, $t\bar{t}$, dibosons VV' and QCD multi-jet components. We quantify the signal sensitivity via a binned log-likelihood analysis to the $\not{E}_T$ distribution, invoking the CL_s method [52]. In Fig. 7 we show the 95% C.L. bound on the (m_a, t_β) plane for $\mathcal{L} = 100$ fb^{-1}. We stress, however, the strong impact of systematic uncertainties on the mono-jet bounds: as shown in Fig. 7 (dashed-line), including the 5% background systematic uncertainty [53,54] weakens the mono-jet sensitivity to $t_\beta \lesssim 0.6$, below the flavor bound for 2HDM Type I.

C. LHC phenomenology: Mono-Z searches

We now analyze the $pp \to Za$ channel. This channel can produce a very distinct collider signature characterized by boosted leptonic Z decays recoiling against large amounts of missing energy from the a decays to dark matter $a \to \bar{\chi}\chi$ [28,55]; see Fig. 5. The main backgrounds for this signature are top pair $\bar{t}t +$ jets, diboson pair $V^{(*)}V'^{(*)} = WW$, ZZ, WZ and $Z +$ jets production.

We simulate our signal and background samples with SHERPA+OPENLOOPS [42,43,55,56]. The diboson and top-pair samples are generated with the MEPS@NLO algorithm with up to one extra jet emission and the $Z +$ jets with the same method merging up to two jets [57]. We also include the loop-induced gluon fusion contributions that arise for ZZ and WW production [55]. They are simulated at LO accuracy merged via the CKKW algorithm up to one extra jet [44]. Spin correlations and finite width effects from the vector bosons are accounted for in our simulation, as well as hadronization and underlying event effects [58]. The pseudoscalar a and heavy scalar H widths are calculated from HDECAY [59].

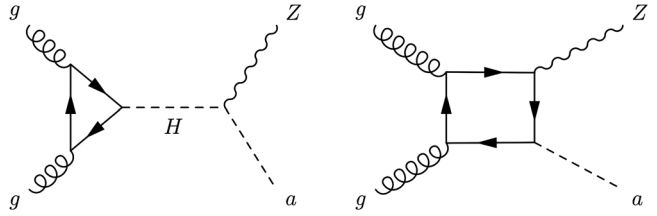

FIG. 5. Sample of Feynman diagrams for the signal $gg \to Za$.

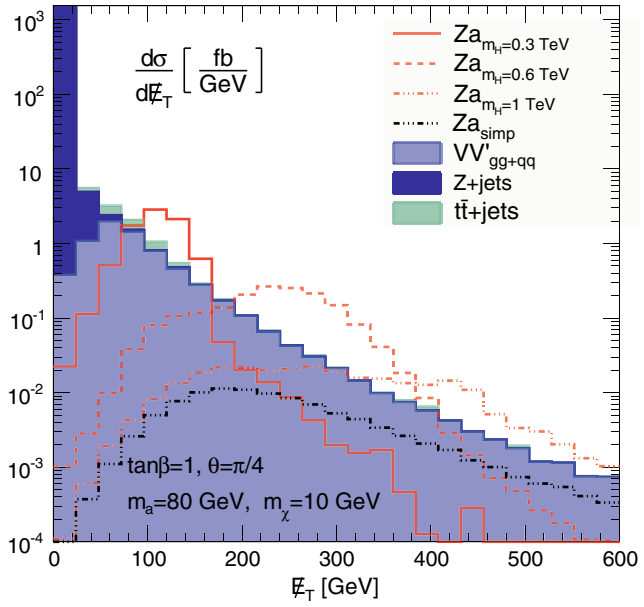

FIG. 6. Signal (red) and background (blue/green) $\not{E}_T$ distributions for $m_\chi = 10$ GeV, $\sin^2(\theta) = 1/2$, $\tan\beta = g_\chi = 1$ and $m_a = 80$ GeV (with $m_A \gg m_a$). Shaded (empty) histograms are (non) stacked. We display the signal scenarios $m_H = 0.3$, 0.6, 1 TeV (red) and within the simplified model framework (black).

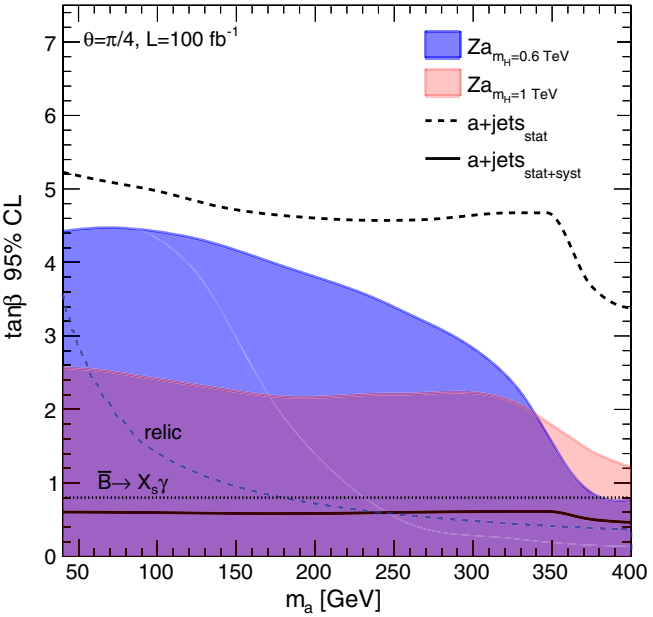

FIG. 7. 95% C.L. bound on $\tan\beta$ as a function of the pseudoscalar mass m_a for the 13 TeV LHC with $\mathcal{L} = 100$ fb^{-1}. We assume $\theta = \pi/4$, $g_\chi = 1$ and a 2HDM Type I in the regime $m_A \gg m_a$. The a + jets bound is displayed in two scenarios: 5% systematic uncertainties on the background (black-full) and with only statistical uncertainties (black-dashed). We also show the lower bound on t_β from $\bar{B} \to X_s\gamma$ (dotted-black) and the relic density curve (dashed-blue) for $m_\chi = 0.4 \times m_a$.

We stress that the loop-induced background and the multi-jet merging signal and background were not accounted for by the experimental analyses so far, and have been shown to be important in related analyses.[5] For this reason, we have resorted to the full Monte Carlo machinery carefully presented in Refs. [55,56] for a more robust prediction.

For the analysis, we require two same-flavor opposite-sign leptons with $p_T^\ell > 20$ GeV, $|\eta_\ell| < 2.5$ and $|m_{\ell\ell} - m_Z| < 15$ GeV. As most of the sensitivity is in the boosted kinematics, $\not{E}_T \gtrsim 100$ GeV, where the Z boson–decay products are more collimated, we impose that $\Delta\phi_{\ell\ell} < 1.7$. Jets are defined via the anti-k_T jet algorithm $R = 0.4$, $p_{Tj} > 30$ GeV and $|\eta_j| < 5$. To tame the $t\bar{t}$ + jets background, we consider only the zero and one-jet exclusive bins vetoing extra jet emissions and b-tagged jets. In Fig. 6 the resulting $\not{E}_T$ distributions are shown, which highlights that for $\not{E}_T \gtrsim 90$ GeV, the backgrounds Z + jets and $t\bar{t}$ + jets get quickly depleted and the diboson VV' becomes dominant.

Remarkably, for $m_H > m_a + m_Z$, H can be resonantly produced yielding a maximum in the $\not{E}_T$ spectrum [28]

$$\not{E}_T^{\max} \sim \frac{1}{2m_H}\sqrt{(m_H^2 - m_a^2 - m_Z^2)^2 - 4m_Z^2 m_a^2}. \quad (12)$$

[5]The impact of the loop-induced components to 13 TeV LHC tantamount to a correction of ~30% in the Higgs boson $\mathcal{BR}(H \to \text{inv})$ bounds [55].

The position of the peak can then be shifted by changing m_H. In Fig. 6 we show the $m_H = 0.3$, 0.6, 1 TeV scenarios, that peak respectively at $\not{E}_T^{\max} \sim 125$, 280, 490 GeV, following Eq. (12). Noticeably, the peak gets less pronounced for larger m_H due to the larger heavy resonance width Γ_H, smearing it out.

The 95% C.L. signal sensitivity on the (m_a, t_β) plane for the $m_H = 0.6$, 1 TeV benchmarks, through a two-dimensional ($\not{E}_T$ vs. number of jets $n_j = 0$, 1) binned log-likelihood, using the CLs method [52] with a 10% systematic uncertainty on the background rate [60], is shown in Fig. 7 for $\mathcal{L} = 100$ fb^{-1}. For comparison, Fig. 7 also shows the 95% C.L. signal sensitivity on the (m_a, t_β) plane from the mono-jet search for background systematic uncertainties of order 5% (as is the case in current experimental analyses [53,54]) and assuming only statistical uncertainties on the background. The uncertainties are modeled as nuisance parameters in all cases. Finally, we also include in Fig. 7 the 2HDM Type I lower bound $t_\beta \gtrsim 0.8$ (for $m_{H^\pm} = 1$ TeV) from $\bar{B} \to X_s\gamma$ and the relic density curve assuming $m_\chi = 0.4 \times m_a$.

The results from Fig. 7 stress that DM phenomenology at the LHC for the pseudoscalar portal is very different for simplified model and consistent completion, particularly due to the presence of H in the latter (and also A, $H^\pm$ if light), which are within LHC reach due to unitarity bounds

in the phenomenologically relevant case $s_\theta \neq 0$. In this respect, mono-Z searches yield a significantly higher reach than mono-jet searches within the pseudoscalar portal if present background systematic uncertainties are considered. Fig. 7 also highlights that mono-Z searches have a strong potential to probe into the parameter space yielding the correct relic density. Furthermore, for $m_\chi > m_a/2$, the mediator a decays dominantly into SM particles (e.g. $a \to \bar{b}b$), and the process $pp \to H \to Za$ also provides the leading probe of the mediator a [26,39,61]), complementing the associated pseudoscalar top channel $pp \to t\bar{t}a$ [62,63] and significantly increasing the sensitivity of LHC searches to the parameter space region with $m_\chi > m_a/2$.

IV. SUMMARY

In this paper we have analyzed a minimal UV completion of the simplified pseudoscalar dark matter portal scenario. In a minimal consistent setup, mixing between the light pseudoscalar and the new degrees of freedom (needed for the existence of the portal) combined with unitarity of scattering amplitudes require the new states to be around the TeV scale or below. This leads to key LHC phenomenology beyond the simplified model in the form of mono-Z signatures, which yield a stronger sensitivity than the generic mono-jets analysis. Such an outcome evinces the limitations of simplified models which are not gauge-invariant, and it evidences that the omission of degrees of freedom required for the theoretical consistency of simplified models can lead to a generic failure of these scenarios to capture the relevant physics.

ACKNOWLEDGMENTS

We are grateful to the Mainz Institute for Theoretical Physics (MITP) and the Universidade de São Paulo for the hospitality and partial support. We also thank Tilman Plehn and Carlos Savoy for very useful discussions, and Patrick Fox and Ayres Freitas for comments on the manuscript. The work of D. G. was funded by STFC through the IPPP grant and U.S. National Science Foundation under Grant No. PHY-1519175. This project has received funding from the Centro de Excelencia Severo Ochoa Grant No. SEV-2012-0249 (PM), and the following EU grants: People Programe (FP7/2007–2013) Grant No. PIEF-GA-2013-625809 EWBGLHC (JMN); H2020 ERC Grant Agreement No. 648680 DARKHORIZONS (JMN); Grant No. FP7 ITN INVISIBLES PITN-GA-2011-289442 (PM); Grant No. H2020-MSCA-ITN-2015/674896-Elusives (PM); Grant No. H2020-MSCA-2015-690575-InvisiblesPlus (PM). Fermilab is operated by the Fermi Research Alliance, LLC under Contract No. DE-AC02-07CH11359 with the United States Department of Energy.

[1] G. Bertone, D. Hooper, and J. Silk, Phys. Rep. **405**, 279 (2005).
[2] B. Patt and F. Wilczek, arXiv:hep-ph/0605188; S. Andreas, T. Hambye, and M. H. G. Tytgat, J. Cosmol. Astropart. Phys. 10 (2008) 034; J. March-Russell, S. M. West, D. Cumberbatch, and D. Hooper, J. High Energy Phys. 07 (2008) 058; L. Lopez-Honorez, T. Schwetz, and J. Zupan, Phys. Lett. B **716**, 179 (2012); A. Djouadi, O. Lebedev, Y. Mambrini, and J. Quevillon, Phys. Lett. B **709**, 65 (2012); Y. G. Kim, K. Y. Lee, and S. Shin, J. High Energy Phys. 05 (2008) 100; C. Englert, T. Plehn, D. Zerwas, and P. M. Zerwas, Phys. Lett. B **703**, 298 (2011); A. Freitas, S. Westhoff, and J. Zupan, J. High Energy Phys. 09 (2015) 015.
[3] J. Abdallah *et al.*, arXiv:1409.2893.
[4] M. R. Buckley, D. Feld, and D. Goncalves, Phys. Rev. D **91**, 015017 (2015).
[5] A. De Simone and T. Jacques, Eur. Phys. J. C **76**, 367 (2016).
[6] S. Matsumoto, S. Mukhopadhyay, and Y. L. S. Tsai, J. High Energy Phys. 10 (2014) 155.
[7] A. Alves, S. Profumo, and F. S. Queiroz, J. High Energy Phys. 04 (2014) 063.
[8] S. Matsumoto, S. Mukhopadhyay, and Y. L. S. Tsai, Phys. Rev. D **94**, 065034 (2016).
[9] G. Busoni, A. De Simone, E. Morgante, and A. Riotto, Phys. Lett. B **728**, 412 (2014).
[10] O. Buchmueller, M. J. Dolan, and C. McCabe, J. High Energy Phys. 01 (2014) 025.
[11] G. Busoni, A. De Simone, J. Gramling, E. Morgante, and A. Riotto, J. Cosmol. Astropart. Phys. 06 (2014) 060.
[12] A. Choudhury, K. Kowalska, L. Roszkowski, E. M. Sessolo, and A. J. Williams, J. High Energy Phys. 04 (2016) 182.
[13] F. Kahlhoefer, K. Schmidt-Hoberg, T. Schwetz, and S. Vogl, J. High Energy Phys. 02 (2016) 016.
[14] C. Englert, M. McCullough, and M. Spannowsky, Phys. Dark Univ. **14**, 48 (2016).
[15] M. Duerr, F. Kahlhoefer, K. Schmidt-Hoberg, T. Schwetz, and S. Vogl, J. High Energy Phys. 09 (2016) 042.
[16] A. Boveia *et al.*, arXiv:1603.04156.
[17] M. Bauer *et al.*, arXiv:1607.06680.
[18] A. Ismail, W. Y. Keung, K. H. Tsao, and J. Unwin, arXiv:1609.02188.
[19] N. F. Bell, Y. Cai, and R. K. Leane, J. Cosmol. Astropart. Phys. 01 (2017) 039.
[20] U. Haisch, F. Kahlhoefer, and J. Unwin, J. High Energy Phys. 07 (2013) 125.
[21] P. J. Fox and C. Williams, Phys. Rev. D **87**, 054030 (2013).

[22] P. Harris, V. V. Khoze, M. Spannowsky, and C. Williams, Phys. Rev. D **91**, 055009 (2015).
[23] U. Haisch, A. Hibbs, and E. Re, Phys. Rev. D **89**, 034009 (2014).
[24] O. Mattelaer and E. Vryonidou, Eur. Phys. J. C **75**, 436 (2015).
[25] S. Ipek, D. McKeen, and A. E. Nelson, Phys. Rev. D **90**, 055021 (2014).
[26] D. Gonçalves, P. A. N. Machado, and J. M. No (to be published).
[27] Y. Nomura and J. Thaler, Phys. Rev. D **79**, 075008 (2009).
[28] J. M. No, Phys. Rev. D **93**, 031701 (2016).
[29] J. F. Gunion and H. E. Haber, Phys. Rev. D **67**, 075019 (2003).
[30] G. C. Branco, P. M. Ferreira, L. Lavoura, M. N. Rebelo, M. Sher, and J. P. Silva, Phys. Rep. **516**, 1 (2012).
[31] G. Aad *et al.* (ATLAS Collaboration), J. High Energy Phys. 11 (2015) 206.
[32] W. Grimus, L. Lavoura, O. M. Ogreid, and P. Osland, J. Phys. G **35**, 075001 (2008).
[33] J.-M. Gerard and M. Herquet, Phys. Rev. Lett. **98**, 251802 (2007).
[34] S. Kanemura, T. Kubota, and E. Takasugi, Phys. Lett. B **313**, 155 (1993).
[35] A. G. Akeroyd, A. Arhrib, and E. M. Naimi, Phys. Lett. B **490**, 119 (2000).
[36] I. F. Ginzburg and I. P. Ivanov, Phys. Rev. D **72**, 115010 (2005).
[37] B. Grinstein, C. W. Murphy, and P. Uttayarat, J. High Energy Phys. 06 (2016) 070.
[38] F. Kling, J. M. No, and S. Su, J. High Energy Phys. 09 (2016) 093.
[39] G. C. Dorsch, S. J. Huber, K. Mimasu, and J. M. No, Phys. Rev. D **93**, 115033 (2016).
[40] T. Hermann, M. Misiak, and M. Steinhauser, J. High Energy Phys. 11 (2012) 036.
[41] M. Misiak *et al.*, Phys. Rev. Lett. **114**, 221801 (2015).
[42] T. Gleisberg, S. Höche, F. Krauss, M. Schönherr, S. Schumann, F. Siegert, and J. Winter, J. High Energy Phys. 02 (2009) 007; F. Krauss, R. Kuhn, and G. Soff, J. High Energy Phys. 02 (2002) 044; T. Gleisberg and S. Hoeche, J. High Energy Phys. 12 (2008) 039; T. Gleisberg and F. Krauss, Eur. Phys. J. C **53**, 501 (2008); S. Höche, F. Krauss, M. Schönherr, and F. Siegert, J. High Energy Phys. 09 (2012) 049.
[43] F. Cascioli, P. Maierhöfer, and S. Pozzorini, Phys. Rev. Lett. **108**, 111601 (2012); A. Denner, S. Dittmaier, and L. Hofer, Comput. Phys. Commun. **212**, 220 (2017).
[44] S. Catani, F. Krauss, R. Kuhn, and B. R. Webber, J. High Energy Phys. 11 (2001) 063; F. Krauss, J. High Energy Phys. 08 (2002) 015; S. Hoeche, F. Krauss, S. Schumann, and F. Siegert, J. High Energy Phys. 05 (2009) 053.
[45] M. Buschmann, D. Goncalves, S. Kuttimalai, M. Schonherr, F. Krauss, and T. Plehn, J. High Energy Phys. 02 (2015) 038.
[46] T. Corbett, O. J. P. Eboli, D. Goncalves, J. Gonzalez-Fraile, T. Plehn, and M. Rauch, J. High Energy Phys. 08 (2015) 156.
[47] CMS Collaboration, Report No. CMS-PAS-EXO-15-003, 2015.
[48] M. Cacciari, G. P. Salam, and G. Soyez, J. High Energy Phys. 04 (2008) 063; Eur. Phys. J. C **72**, 1896 (2012).
[49] CMS Collaboration, Report No. CMS-PAS-BTV-13-001, 2013.
[50] C. Oleari, Nucl. Phys. B, Proc. Suppl. **205**–**206**, 36 (2010).
[51] U. Haisch, F. Kahlhoefer, and E. Re, J. High Energy Phys. 12 (2013) 007.
[52] A. L. Read, J. Phys. G **28**, 2693 (2002).
[53] V. Khachatryan *et al.* (CMS Collaboration), Eur. Phys. J. C **75**, 235 (2015).
[54] M. Aaboud *et al.* (ATLAS Collaboration), Phys. Rev. D **94**, 032005 (2016).
[55] D. Goncalves, F. Krauss, S. Kuttimalai, and P. Maierhoefer, Phys. Rev. D **94**, 053014 (2016).
[56] D. Goncalves, F. Krauss, S. Kuttimalai, and P. Maierhoefer, Phys. Rev. D **92**, 073006 (2015).
[57] S. Höche, F. Krauss, M. Schönherr, and F. Siegert, J. High Energy Phys. 04 (2013) 027; T. Gehrmann, S. Höche, F. Krauss, M. Schönherr, and F. Siegert, J. High Energy Phys. 01 (2013) 144.
[58] S. Höhe, S. Kuttimalai, S. Schumann, and F. Siegert, Eur. Phys. J. C **75**, 135 (2015).
[59] A. Djouadi, J. Kalinowski, and M. Spira, Comput. Phys. Commun. **108**, 56 (1998).
[60] CMS Collaboration, Report No. CMS-PAS-HIG-16-016, 2016.
[61] V. Khachatryan *et al.* (CMS Collaboration), Phys. Lett. B **759**, 369 (2016).
[62] D. Goncalves and D. Lopez-Val, Phys. Rev. D **94**, 095005 (2016).
[63] M. Casolino, T. Farooque, A. Juste, T. Liu, and M. Spannowsky, Eur. Phys. J. C **75**, 498 (2015).